LAWRENCE
LIVERMORE
NATIONAL
LABORATORY

LLNL-JRNL-782038

X-ray Observations of Ne-like Xe and Satellites from C-Mod Tokamak Plasmas

J. E. Rice , K. B. Fournier, G. E. Kemp, M. Bitter, N. Cao, L. Delgado-Aparicio, K. Hill, A. E. Hubbard, J. W. Hughes, M. L. Reinke

July 19, 2019

X-ray Observations of Ne-like Xe and Satellites from C-Mod Tokamak Plasmas

X-ray Observations of Ne-like Xe and Satellites from C-Mod Tokamak Plasmas

J.E. Rice, K.B. Fournier[♭], G.E. Kemp[♭], M. Bitter[♮], N. Cao, L. Delgado-Aparicio[♮], K. Hill[♮], A.E. Hubbard, J.W. Hughes and M.L. Reinke[†]

Plasma Science and Fusion Center, MIT, Cambridge, MA, USA

[♮]*Princeton Plasma Physics Laboratory, Princeton, NJ, USA*

[♭]*LLNL, Livermore, CA, USA*

[†]*ORNL*

Abstract

X-ray spectra in the wavelength range from 2.70 to 2.76 Å from xenon (Z = 54) in near neon-like charge states have been observed in Alcator C-Mod tokamak plasmas. The 3D ($2p^6$ - $(2p^5)_{3/2}3d_{5/2}$, 2720.4 mÅ) and 3F ($2p^6$ - $(2p^5)_{1/2}3s_{1/2}$, 2729.0 mÅ) transitions from neon-like Xe^{44+} have been identified, along with nearby Na-, Mg- and Al-like satellites. The intensity ratio of 3D to the Mg-like satellite near 2.74 Å increases strongly with electron temperature in the range from 3 to 4 keV.

I. Introduction

Xenon (Z = 54) is being considered as a species for the ITER x-ray crystal imaging system in order to provide ion temperature and toroidal rotation velocity profiles. In particular, the neon-like charge state Xe^{44+} exists and radiates substantially over an electron temperature range from 3.5 to 10 keV according to calculations [1]. The purpose of these experiments on the Alcator C-Mod tokamak was to measure the x-ray spectrum of Ne-like Xe, make line identifications and obtain experience with Xe puffing, in order to inform decisions about the ITER system.

X-ray spectra of neon-like xenon (and nearby elements), including neighboring satellites, have been obtained from laser produced plasmas [2], tokamaks [3, 4, 5, 6, 7], low inductance sparks [8] and electron beam ion traps [9, 10, 11, 12]. In the present treatment, following a discussion of line identifications, the relative intensities of satellites compared to the xenon neon-like resonance line will be explored as a function of electron temperature.

II. Experimental Setup and Wavelength Calibration

The observations described here were obtained from the Alcator C-Mod tokamak [13], a compact high magnetic field device fitted with molybdenum plasma facing components. With auxiliary radio frequency heating, it is possible to explore a range of electron temperatures at fixed electron density. X-ray spectra were recorded with a spatially imaging high resolution x-ray spectrometer system [14, 15]. In order to view the spectral range between 2.70 and 2.76 Å, a quartz 022 crystal (2d = 3.3396 Å) was utilized, giving rise to a Bragg angle around 55^o. This configuration also covers the K_β spectrum of He-like Ca^{18+} [16, 17] including the 1s3p $^1P_1$ - 1s^2 $^1S_0$ resonance line w_3 at 2.7055 Å and the 1s3p $^3P_1$ - 1s^2 $^1S_0$ intercombination line y_3 at 2.7086 Å, which can provide an accurate wavelength calibration. An example of the calcium spectrum in the same wavelength range [17], following CaF_2 injection from laser blow-off, is shown in Fig.1. w_3 dominates over y_3 by about a factor of 10, dependeing on plasma parameters.

III. Xe Observations

Xenon was introduced into C-Mod plasmas through a piezo-electric valve. A workable setup included a 4:1 mixture of Ar:Xe with a plenum pressure of 2 psi and a pulse of duration 120 ms. An example of parameter time histories for an ICRF heated discharge with a Xe puff is shown in Fig.2. The valve was open from 0.3 to 0.42 seconds, and the total radiated power was seen to respond immediately (third panel). There was no visible x-ray signal ($4^{\rm th}$ frame) until the electron temperature exceeded 3 keV after initiation of 3 MW of ICRF heating power at 0.5 s (second panel). Larger Xe puffs led to disruptions under these conditions.

An x-ray spectrum in the vicinity of the Xe^{44+} 3D line is shown in Fig.3, for a discharge with a central electron temperature of 3 keV and average electron density

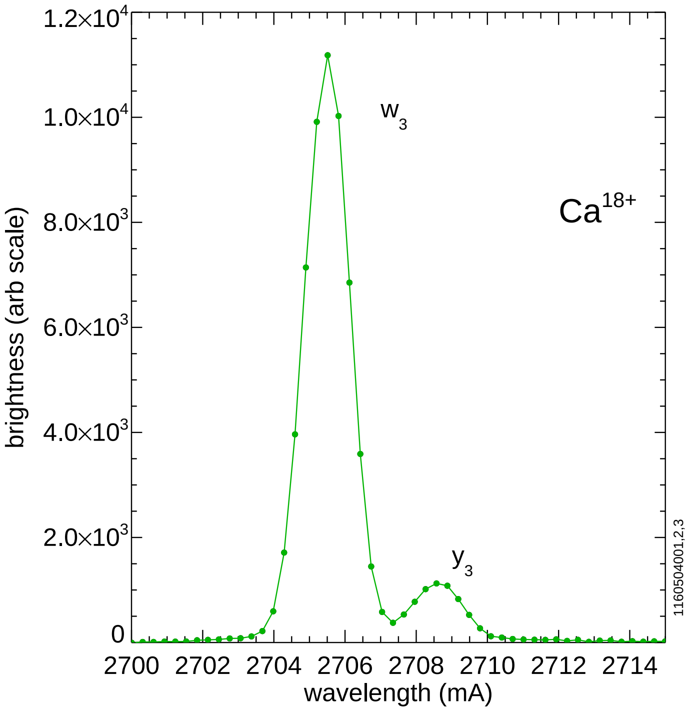

Figure 1: The He-like Ca^{18+} spectrum including the w_3 and y_3 transitions.

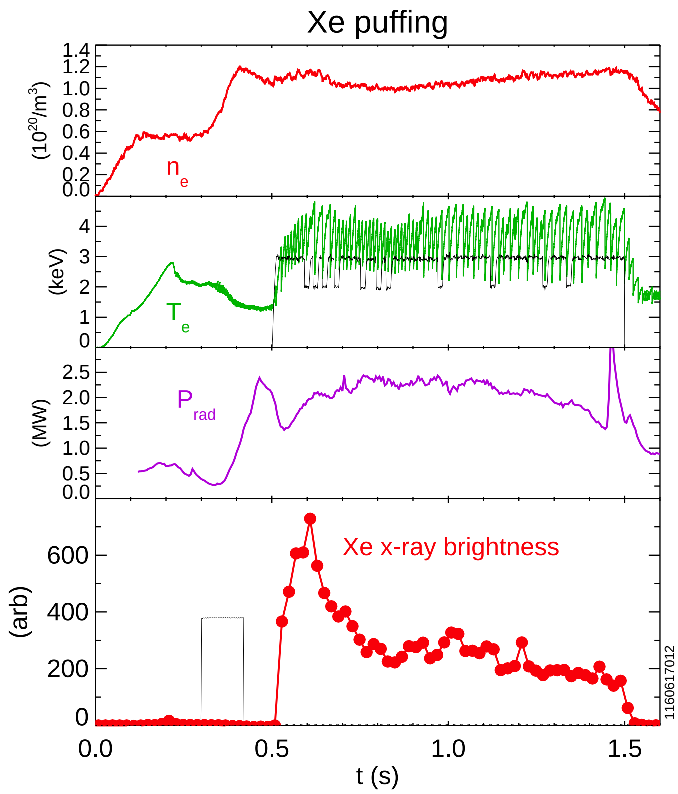

Figure 2: Plasma parameter time histories for an I-mode discharge formed with 3 MW of ICRF power. From top to bottom, the electron density, the central electron temperature (and ICRF power), total radiated power and Xe x-ray brightness between 2.70 and 2.76 Å (and piezo-electric valve waveform).

of $4\times10^{19}/m^3$. The 3D ($2p^6$ - $(2p^5)_{3/2}3d_{5/2}$) and 3F ($2p^6$ - $(2p^5)_{1/2}3s_{1/2}$) transitions

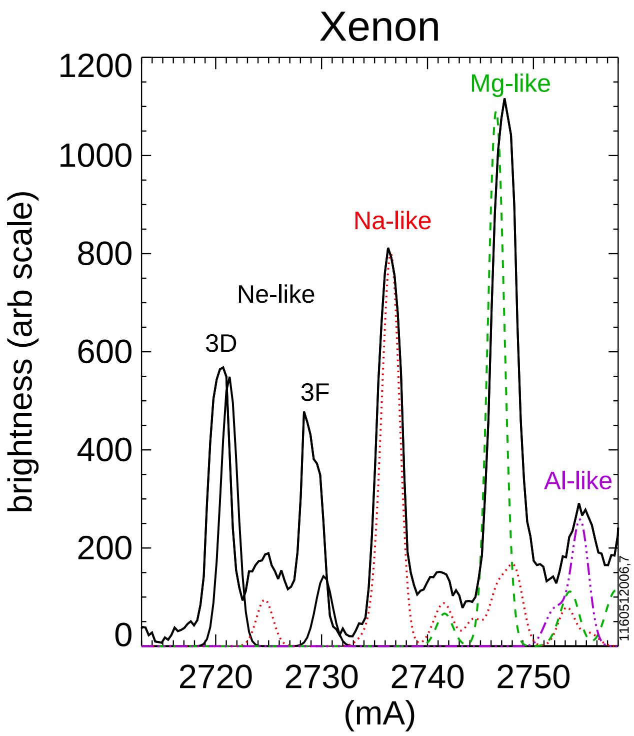

Figure 3: An observed xenon x-ray spectrum in the vicinity of the 3D transition. Synthetic spectra are shown for neon-like (solid black), sodium-like (red dotted), magnesium-like (green dashed) and aluminum-like (purple chain) charge states.

from neon-like Xe^{44+} are clearly identified. The experimental wavelengths of 2720.4 and 2729.0 mÅ, respectively, are in excellent agreement with the results from the PLT tokamak [5]. At this electron temperature, however, Mg- and Na-like satellites, at 2736.4 and 2747.2 mÅ, respectively, are dominant. Calculations from the atomic structure code SCRAM [18] are shown for comparison. The black solid line is the spectrum from neon-like Xe^{44+}, with the red dotted line from sodium-like Xe^{43+}, the green dashed line from magnesium-like Xe^{42+} and the purple chain line from aluminum-like Xe^{41+}, in good agreement with the observations. The results from each individual charge state are normalized to the brightest lines.

Support for the identification of the 3F transition comes from a comparison of the wavelength relative to 3D in different elements. For example, a spectrum in the vicinity of the 3D line in palladium (following Pd injection into C-Mod plasmas) is shown in Fig.4 [6] for 1.8 keV discharges with a density of $1.1\times10^{20}/m^3$. The Na-like Pd^{35+} and Mg-like Pd^{34+} lines relative to the Ne-like Pd^{36+} 3D line appear very similar to

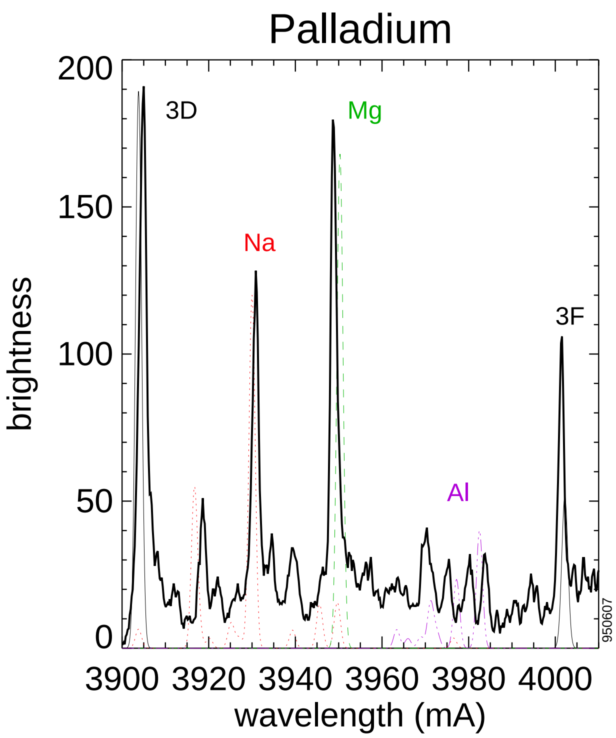

Figure 4: An observed x-ray spectrum in the vicinity of the Pd^{36+} 3D transition. Synthetic spectra are shown for neon-like (solid black), sodium-like (red dotted), magnesium-like (green dashed) and aluminum-like (purple dash-dot) charge states.

the Xe spectrum of Fig.3, whereas the 3F transition is found at a considerably longer wavelength. Synthetic spectra are also shown, with good agreement: Ne-like (solid black), Na-like (red dotted), Mg-like (green dashed) and Al-like (purple dash-dot). The wavelength difference between 3F and 3D indicates a strong variation as a function of atomic number. Shown by the red dots in Fig.5 are the observed normalized wavelength differences $(\lambda_{3F} - \lambda_{3D})/\lambda_{3D}$ as a function of atomic number for elements between palladium (Pd^{36+}) and neodymium (Nd^{50+}) [4, 5, 6, 9]. For comparison are

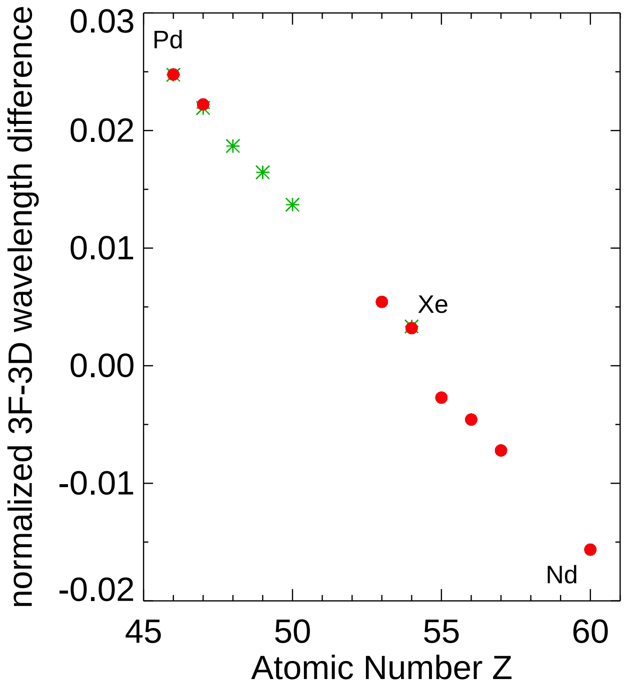

Figure 5: The observed normalized wavelength difference $(\lambda_{3F} - \lambda_{3D})/\lambda_{3D}$ as a function of atomic number are shown as red dots. The calculated wavelength differences are shown as green asterisks.

the calculated values from the RELAC code [19, 20], in excellent agreement. For elements with atomic number above cesium (Cs^{45+}), 3F appears on the short wavelength (high energy) side of 3D. This is due to the increased relativistic energy splitting of the $2p^5{}_{1/2}$ and $2p^5{}_{3/2}$ core configurations in 3F and 3D, respectively. The convergence in wavelength of 3F and 3D with increasing atomic number can be understood through examination of the transition upper level energy scaling. The calculated (from RELAC) energies of the transition upper levels for 3F and 3G converge for xenon (Z=54) as the atomic number is increased.

The wavelength systematic variation with atomic number supports the identification of the line at 2729.1 mÅ in Fig.3 as 3F in Xe^{44+}. In a similar fashion, examination of the satellite wavelengths as a function of atomic charge supports the identification of the strong Na- and Mg-like satellites in Fig.3. Shown in Fig.6 are the observed wavelength differences between the Ne-like 3D transition and the strongest Na- and Mg-like satellites as a function of atomic number for palladium [6], silver [4] and xenon. These

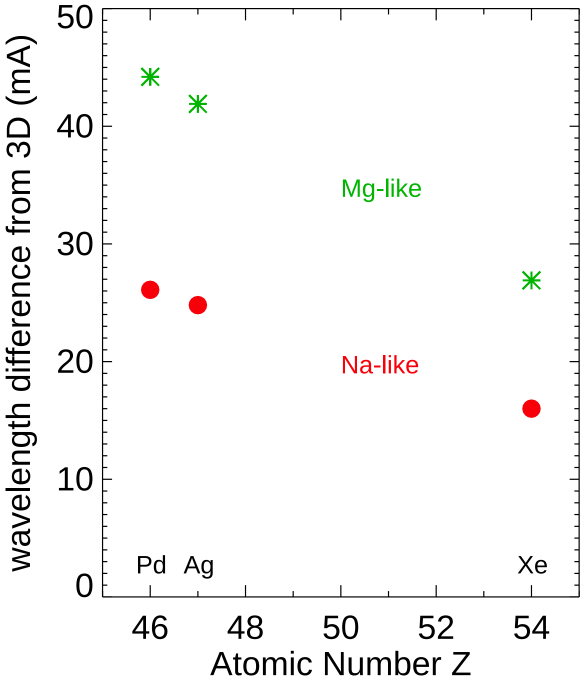

Figure 6: The observed wavelength difference ($\lambda_{sat} - \lambda_{3D}$) between the brightest sodium-like (red dots) and magnesium-like (green asterisks) and the neon-like 3D as a function of atomic number.

wavelength differences vary smoothly with atomic number.

The intensity ratio of the Ne-like 3D transition to the strongest Mg-like satellite line has been investigated as a function of central electron temperature at a fixed density of $1{\times}10^{20}/m^3$, and is shown in Fig.7. This ratio increases strongly as the electron temperature is raised, over the available range, consistent with calculations [1] which show a dramatic rise in the neon-like Xe^{44+} fractional abundance between 3 and 4 keV. At 4 keV this ratio is still not much larger than unity, even though this is about half of the ionization potential of Xe^{44+}. A more suitable ratio for the purposes of plasma diagnostics would be more like 5 to 1, which has been obtained in neon-like krypton

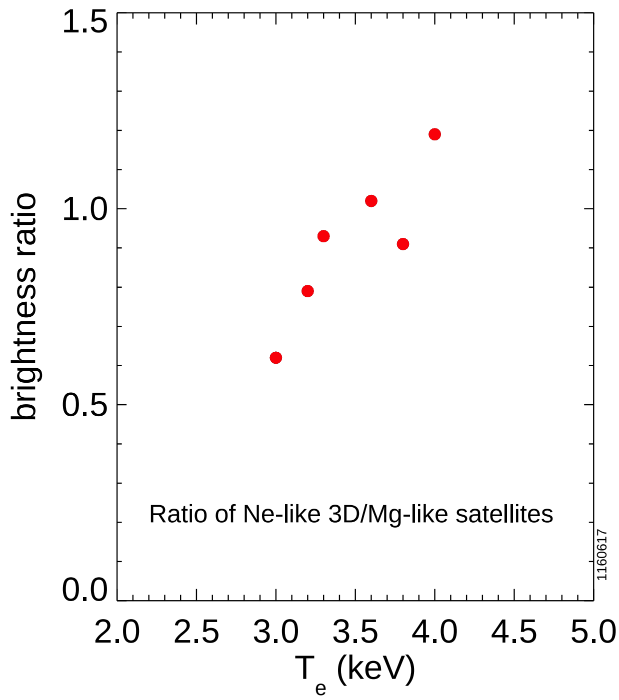

Figure 7: The intensity ratio of the 3D transition to Mg-like satellite line as a function of measured electron temperature.

[7].

IV. Summary and Conclusions

Xenon has been introduced in C-Mod tokamak plasmas by gas puffing and x-ray spectra in the interval 2.70−2.76 Å have been obtained from a high resolution x-ray spectrometer system. The 3D and 3F transitions, at 2720.4 and 2729.0 mÅ, respectively, in Ne-like Xe^{44+} have been identified, along with nearby Na-, Mg- and Al-like satellites. Identification has been made by comparison with collisional-radiative modeling, in addition to a wavelength scaling with atomic number in nearby elements. The ratio of the 3D transition to the strong Mg-like satellites increases strongly with electron temperature between 3 and 4 keV.

V. Acknowledgements

Work supported at MIT by DoE Contract No. DE-FC02-99ER54512 and under the auspices of the U.S. Department of Energy by the Lawrence Livermore National Laboratory under Contract No. DE-AC52-07NA27344.

References

[1] Hu R.J. *et al*, 2018 *Rev. Sci. Instrum.* **89** 10F110.

[2] Conturie Y. *et al.*, 1981 *J. Opt. Soc. Am.* **71** 1309.

[3] Källne E. *et al.*, 1983 *Phys. Rev. A* **27** 2682.

[4] Beiersdorfer P. *et al.*, 1986 *Phys. Rev. A* **34** 1297.

[5] Beiersdorfer P. *et al.*, 1988 *Phys. Rev. A* **37** 4153.

[6] Rice J.E. *et al.*, 1996 *Phys. Rev. A* **53** 3953.

[7] Rice J.E. *et al.*, 2000 *J. Phys. B* **33** 5435.

[8] Aglitskii E.V. *et al.*, 1989 *Phys. Scr.* **40** 601.

[9] Nakamura N. *et al.*, 2000 *Phys. Rev. A* **61** 052510.

[10] Kato D. *et al.*, 2001 *Phys. Scr.* **T92** 126.

[11] Werner T. *et al.*, 2001 *Phys. Scr.* **T92** 241.

[12] Beiersdorfer P. *et al.*, 2009 *Phys. Scr.* **T134** 014010.

[13] Marmar E.S. *et al.*, 2007 *Fusion Sci. Technol.* **51** 261.

[14] Ince-Cushman A. *et al*, 2008 *Rev. Sci. Instrum.* **79** 10E302.

[15] Reinke M.L. *et al*, 2012 *Rev. Sci. Instrum.* **83** 113504.

[16] Vainshtein L.A. and Safronova U.I., 1985 *Phys. Scr.* **31** 519.

[17] Rice J.E. *et al.*, 2018 *J. Phys. B* **51** 035702.

[18] Hansen S.B. *et al.*, 2007 *High Energy Density Phys.* **3** 109.

[19] Klapisch M., 1971 *Comput. Phys. Comm.* **2** 269.

[20] Klapisch M. *et al.*, 1977 *J. Opt. Soc. Am.* **67** 148.